Numerical ensemble study of ergodic properties of the quartic Fermi-Pasta-Ulam chain

B. I. Henry* and J. Grindlay
Guelph-Waterloo Program for Graduate Work in Physics, Waterloo Campus, University of Waterloo, Waterloo, Ontario, Canada N2L 3G1
(Received 29 January 1988)

A numerical integration of the equations of motion of a 17-particle chain with nearest-neighbor linear and cubic forces has been carried out in quadruple-precision FORTRAN over a period of 600 model time units. The chain has clamped ends and is excited initially in the 11th mode. The data obtained from the integration constitute a reversible time ensemble. Equilibrium mode energy distributions in this ensemble prove to have a Maxwell-Boltzmann form, and in addition the calculated mode temperatures agree with those obtained from the double-precision statistical ensemble previously reported for the same system and same model parameters [B. I. Henry and J. Grindlay, Physica D **28**, 49 (1987)]. It follows that statistical-ensemble averages and time-ensemble averages are equal, and hence the ergodic hypothesis holds for these two data banks.

I. INTRODUCTION

In an earlier paper[1] we introduced a constant energy ensemble for an isolated chain of 17 (15 + 2 in the usual nomenclature) particles with nearest-neighbor linear and cubic forces. The ensemble was constructed by storing the data obtained from a numerical integration of the equations of motion of the particles over a fixed time period for a set of 101 different starting conditions. For each of these system histories the chain was excited at $t=0$ via the 11th mode.[1] Different histories were obtained by choosing different proportions of initial kinetic and potential energies subject to the constraint of a common net starting energy for all the histories. The system was strongly nonlinear in the sense that on average about 18% of the system energy was anharmonic. The numerical integration was carried out in double-precision FORTRAN to give reversible histories accurate to better than 0.02% in the total energy over a time period of 250 sec. To analyze the ensemble data we calculated the time-dependent coarse-grained energy distribution for each mode. The resulting mode Boltzmann H functions in the period of 250 sec exhibited a common behavior. Each H function dropped to a minimum in the first 200 sec, and aside from small fluctuations, maintained this value for the remaining 50 sec. We interpreted this as evidence that each mode, and hence the total system, had reached statistical equilibrium reversibly (because the histories are all reversible) in the last 50 sec. Given an equilibrium state in which the mode H functions are at minima and the total energy of the system is a constant, one can then show algebraically that the corresponding coarse-grained equilibrium energy distribution should exhibit a Maxwell-Boltzmann form, with, in general, different temperatures for different modes. An analysis of our ensemble data verified that this is indeed a property of the system; the calculated mode temperatures ranged over two orders of magnitude.

In this paper we report the results of recalculating one of these earlier histories in quadrupole precision rather than double precision. This procedure gives reversible data over the larger time interval (0,600). Treating the single history as a "time ensemble,"[2] we have calculated the coarse-grained mode energy distributions in the statistical equilibrium interval (200,600). These distributions also prove to be Maxwell-Boltzmann in form and moreover the corresponding mode temperatures agree very well with the mode temperatures obtained from the statistical ensemble reported before.[1] Thus we have for the first time to our knowledge numerical evidence for a form of ergodic hypothesis, namely, the equality of statistical ensemble averages and time ensemble averages. We say "form" because first of all we are dealing with averages over finite-time and finite-sized statistical ensembles and not the infinite ranges used in the usual discussion.[3,4] Secondly, limitations are imposed by truncation and roundoff errors and as a result the ergodic property seen in the two data banks can only be indirectly ascribed to the equations of motion. The ergodic hypothesis plays a central role in the foundations of statistical mechanics.[3,4] The question of its validity for physical systems is a classic, unsolved problem in this field and has been discussed over the years by many authors (see Ref. 4 for a list of references). However, these discussions have always been based on algebraic arguments and, to our knowledge, no one has previously attempted a numerical test of the equality of statistical-ensemble and time-ensemble averages.

Our 15 + 2 chain is an example of an isolated system of coupled oscillators with nonintegrable potential-energy terms in the Hamiltonian. A large number of numerical experiments have been performed by previous authors on similar nonintegrable models, and on the basis of these experiments the following properties are believed to be generic. (i) Ordered (quasiperiodic) motions occur close to the invariant Kolmogorov-Arnold-Moser (KAM) tori of the unperturbed system if the energy associated with the perturbation is small relative to the total energy of the system.[5] (ii) Regions corresponding to ordered motions and regions corresponding to irregular motions

coexist on the constant-energy surface if the energy associated with the perturbation is more than a few percent of the total energy of the system.[6–9] These regions, which are accessed by different initial conditions but the same energy, are sometimes referred to as "islands" and "seas," respectively.[6] The seas are characterized by an exponential divergence of initially nearby trajectories in the system phase space. (iii) As the energy associated with the perturbation is further increased, relative to the total system energy, the islands break up and the irregular regions cover an increasing portion of the constant-energy surface.[10] Several disjoint seas may exist that are accessed by different sets of initial conditions.[8,9,11]

The seas referred to above are believed to be ergodic, although no direct evidence has been given previously. The numerical results reported in this paper provide evidence for an ergodic region or sea on the constant-energy surface $E_0=10$ for the Fermi-Pasta-Ulam chain with nearest-neighbor linear and cubic forces. It seems likely that this property too is a generic feature of perturbed oscillator systems.

In Sec. II we describe the model and the numerical time-ensemble data. Total-energy errors and even-mode-energy errors are discussed and evidence is presented for the Maxwell-Boltzmann form. Section III contains a description of the errors in the position and velocity coordinates of the particles and a discussion of the limitations these errors place on the conclusions we draw from our data.

II. MODEL

Consider a (15 + 2)-particle chain with particle labels $n=0,1,2,\ldots,16$. We assume clamped ends and nearest-neighbor linear and cubic forces. If we denote the displacement of the nth particle by x_n, then the boundary conditions and equations of motion can be written in the form[1]

$$x_0 \equiv x_{16} \equiv 0 \ , \tag{1}$$

$$\ddot{x}_n = (x_{n+1}-2x_n+x_{n-1}) + \mu[(x_{n+1}-x_n)^3-(x_n-x_{n-1})^3] \tag{2}$$

for $n=1,2,\ldots,15$. It is convenient to introduce the normal-mode transformation

$$q_s=[2/(N+1)]^{1/2}\sum_{n=1}^{N} x_n \sin[sn\pi/(N+1)] \ , \qquad s=1,2,3,\ldots,N, \quad N=15 \tag{3}$$

with normal-mode frequencies

$$\omega_s = 2\sin[s\pi/2(N+1)] \ . \tag{4}$$

The total energy of the system E_0, say, can be partitioned among the modes to give mode energies[1]

$$\varepsilon_s=\dot{q}_s^{\,2}/2+\omega_s^2 q_s^2/2+\mu/4\sum_{i=1}^{N}\sum_{j=1}^{N}\sum_{k=1}^{N} A_{s,i,j,k} q_s q_i q_j q_k \ , \tag{5}$$

where

$$A_{ijkl}=\frac{1}{2(N+1)}\omega_i\omega_j\omega_k\omega_l(B_{i,j,k,l}+B_{i,j,k,-l}+B_{i,j,-k,l}+B_{i,-j,k,l}+B_{i,j,-k,-l}+B_{i,-j,-k,l}+B_{i,-j,k,-l}+B_{i,-j,-k,-l}) \ , \tag{6}$$

with

$$B_{i,j,k,l}=\begin{cases} 1 & \text{if } i+j+k+l=0 \\ -1 & \text{if } i+j+k+l=\pm 2(N+1) \\ 0 & \text{otherwise} \ . \end{cases} \tag{7}$$

The vanishing of some A_{ijkl} provides selection rules for the transfer of energy among the modes. The mode energies defined in (5) are not necessarily positive; their sum, E_0, is a constant of the motion.

Using quadruple-precision FORTRAN we have carried out a numerical integration of the equations of motion (2) for the case $\mu=0.8$, total energy $E_0=10$, and initial condition $q_{11}=q^0$, where q^0 is a solution of

$$[\mu A_{11,11,11,11}(q^0)^4+2\omega_{11}^2(q^0)^2]=4E_0 \tag{8}$$

and $\dot{q}_{11}$ and all other $q_s,\dot{q}_s$ zero. This is the initial condition labeled $j=0$ in Ref. 1. We used a predictor-corrector multistep method[12,13] with a time step of 10^{-2} sec. The total energy is conserved to better than 0.02% over the length of our computing run, see Fig. 1. Integration errors in the x_n lead, in time, to the appearance of forbidden even modes—forbidden by the A-selection rules for this type of excitation.[1] The time dependence of this total-even-mode-energy error as a fraction of E_0 is also shown in Fig. 1. An earlier analysis of this system[1] has shown that at times beyond the crossover point of these two error curves the numerical data are no longer accurately time reversible, i.e., if at some instant in this later regime we reverse all the particle velocities and continue the numerical integration, then the system does not accurately retrace its motion back to the initial $t=0$ conditions as it should. Since reversibility is a basic property of the equations of motion (2), we have not used the non-

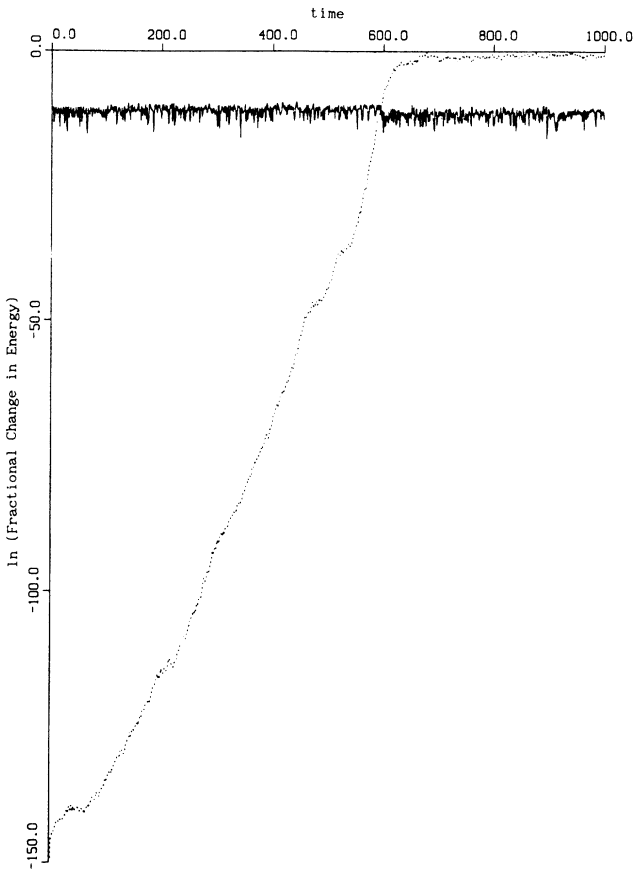

FIG. 1. Graph of energy errors vs time. Solid curve, ln (fractional error in total energy system). Dotted curve, ln (energy in even modes per total energy of system). The data are plotted starting at $t=\frac{1}{10}$ to avoid the logarithmic singularities at $t=0$. Data are from a quadruple-precision integration.

time-reversible data (beyond the crossover point of 600 sec) in the time ensemble described below. Graphs of mode energies ε_s for all the odd modes in the time interval (0,1000) are shown in Fig. 2. As before,[1] the single-history mode-energy data fluctuates to too great an extent (Fig. 2) to permit us to identity an equilibrium regime. The double-precision statistical-ensemble data of 101 histories[1] showed evidence of a statistical equilibrium regime starting at 200 sec and continuing to the end of the run at 250 sec (where on average the 101 even-mode-energy curves in that case cut the total energy error curve). Based on this result we have assumed that in the quadrupole-precision single-history case the statistical equilibrium region extends from 200 sec to the crossover point at 600 sec in Fig. 1. The vertical dotted lines in Fig. 2 indicate these two times. We interpret the data in the three time intervals as describing (i) an initial approach to equilibrium, (ii) a statistical equilibrium state 400 sec long, and (iii) a final nonphysical state determined by the dynamics of the particles, Eq. (2), the choice of algorithm, and the flow of round-off error into the numerical integration procedure. The data in this latter state show some evidence that all modes, both odd and even, tend towards states with a common average energy (see comments below). There is no suggestion of equipartition of energy among the odd modes in the *reversible* equilibrium regime.

We stored the particle position and velocity coordinates at 10^{-1}-sec intervals for 1000 sec. The set of 6001 reversible data points in the time interval (0,600) constitutes our time ensemble. We have no direct algebraic argument to suggest that the 4001 data points in the equilibrium time interval (200,600) would reveal a Maxwell-Boltzmann distribution in the time histories of the energies of the modes. However, given the evidence of this type of distribution in the statistical ensemble,[1] the ergodic hypothesis[3,4] suggests that a test for such a distribution in the time series might prove positive. The analysis was carried out as follows. For the sth mode we partitioned the energy interval $(0,E_0)$ into N_s equal segments[1] (each mode history shows a small incidence of negative mode-energy occurrences, similar in frequency to the same phenomenon in the statistical-ensemble data,[1] see Table I). The incidence is so small that we have neglected these data points in our partitioning process (see discussion in Ref. 1). At each of the 4001 sample points the sth mode has a certain energy. These 4001 points are distributed among the N_s partitions according to this energy, thus giving a coarse-grained energy distribution described by $n_{i,s}$, the number of samples of the sth mode in the ith partition. To the ith partition we ascribe an energy

$$\varepsilon_{i,s}=(i-1/2)E_0/N_s, \quad i=1,2,3,\ldots,N_s \ . \tag{9}$$

If the distribution is Maxwell-Boltzmann in form, then

$$n_{i,s}=C_s\exp(-\varepsilon_{i,s}/\Theta_s) \ , \tag{10}$$

with C_s a normalization constant and Θ_s the mode temperature. Thus $\ln n_{i,s}$ should be a straight-line function of i with slope $-E_0/N_s\Theta_s$. The corresponding $\ln n_{i,s}$ versus i histograms calculated from our numerical data are shown in Fig. 3 for each of the odd modes. The analysis leading to the Maxwell-Boltzmann form[1] (10), suggests that $n_{i,s}$ values less than 20 should be neglected. The remaining points are marked with a cross and fitted to the dashed straight line. These graphs, Fig. 3, provide us with the evidence that the equilibrium mode-energy distribution in the time ensemble is indeed Maxwell-Boltzmann in form. The slopes of the fitted lines give the temperatures Θ_s shown in Table II. (We use the bar to indicate time-ensemble quantities and the brackets for statistical-ensemble quantities.) The statistical-ensemble mode temperatures[1] are shown in the same table for comparison.[14] Aside from the $s=1$ case (where the mode energies are on average very small), the agreement between the two ensemble mode temperatures is good. Thus we conclude that the equilibrium sampling of the constant-energy surface by the 101 copies[1] and the equilibrium sampling of the same surface by the long single history yield the same mode-energy distribution functions. It follows then that time averages over the long single-history

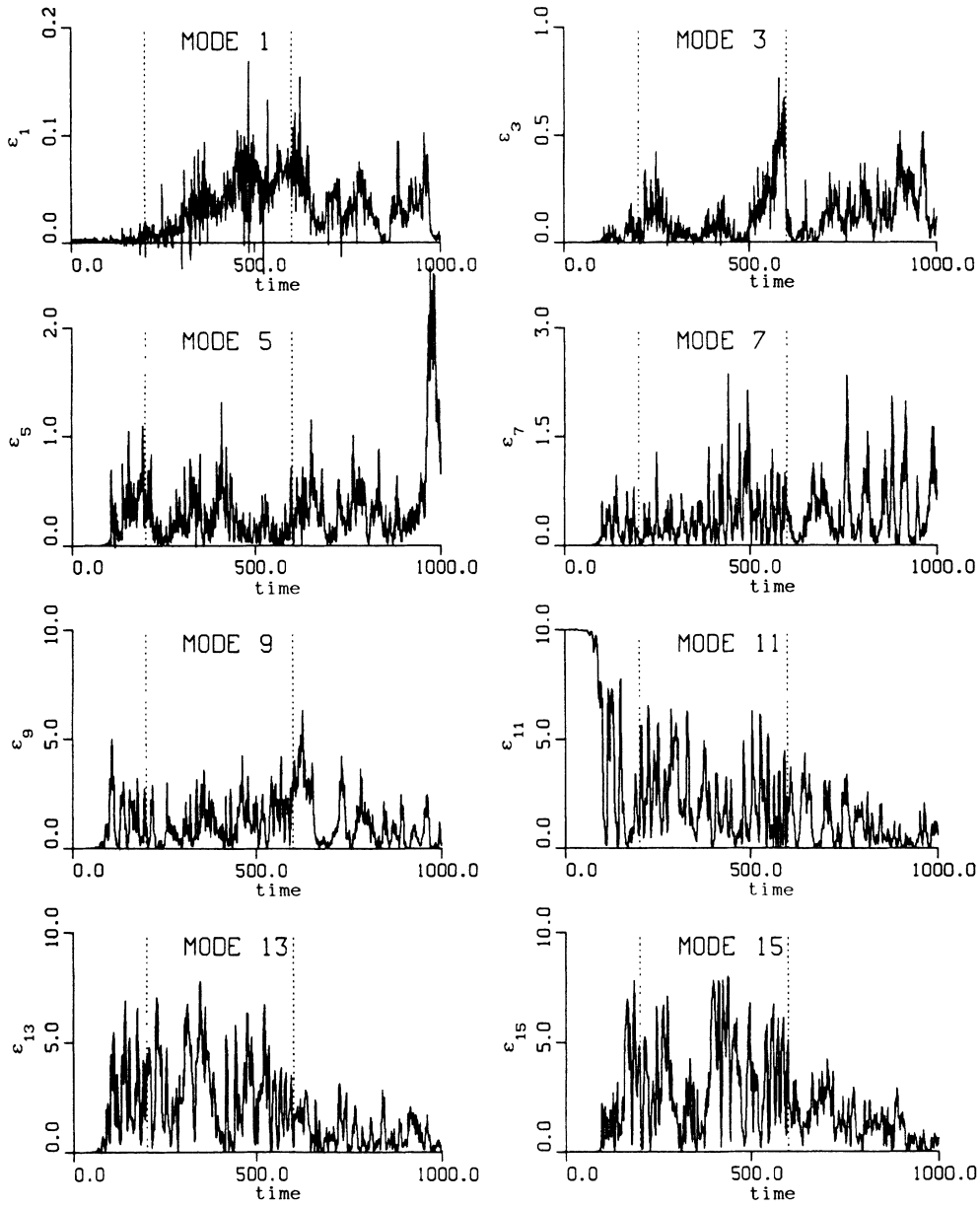

FIG. 2. Graph of ε_s vs time for each of the odd modes $s=1,3,\ldots,15$. The dotted vertical lines at $t=200$ and 600 partition the curves into (i) induction regime (0,200), (ii) equilibrium regime (200,600), and (iii) numerically contaminated regime (600,1000). Note that the energy scales are different for each of the modes.

TABLE I. Fractional number of occurrences of negative energy values <-0.002 for each of the odd modes in the statistical-equilibrium-regime (a) time ensemble in the range [200,600] with 4001 data points, (b) statistical ensemble in the range [200,250] with 5151 data points.

s	(a)	(b)
1	2.4	5.3
3	1.5	1.8
5	0.8	0.5
7	0.3	0.4
9	0.02	0.1
11	0.2	0.06
13	0.07	0.06
15	0.1	0.06

and statistical-ensemble averages over the 101 histories for functions of mode energies should be the same, i.e., a form of the ergodic hypothesis holds for these functions (see remarks in the Introduction). To confirm this conclusion we have calculated the average mode energies $\bar{\varepsilon}_s, \langle \bar{\varepsilon}_s \rangle$, Table II. The numbers agree to the degree that we would expect from the mode temperature comparison. We have not investigated the distribution function for any other physical quantity of this system.[15] However, we have calculated the average value of (a) the mode kinetic energies, written as kinetic temperatures $\bar{\Theta}_s^k = \bar{q}_s^2$ and $\langle \bar{\Theta}_s^k \rangle = \langle \bar{q}_s^2 \rangle$ and (b) particle kinetic energies also written as kinetic temperatures $\bar{T}_n^k = \bar{x}_n^2$ and $\langle \bar{T}_n^k \rangle = \langle \bar{x}_n^2 \rangle$, see Tables III and IV. The numerical agreement between these averages is consistent with the

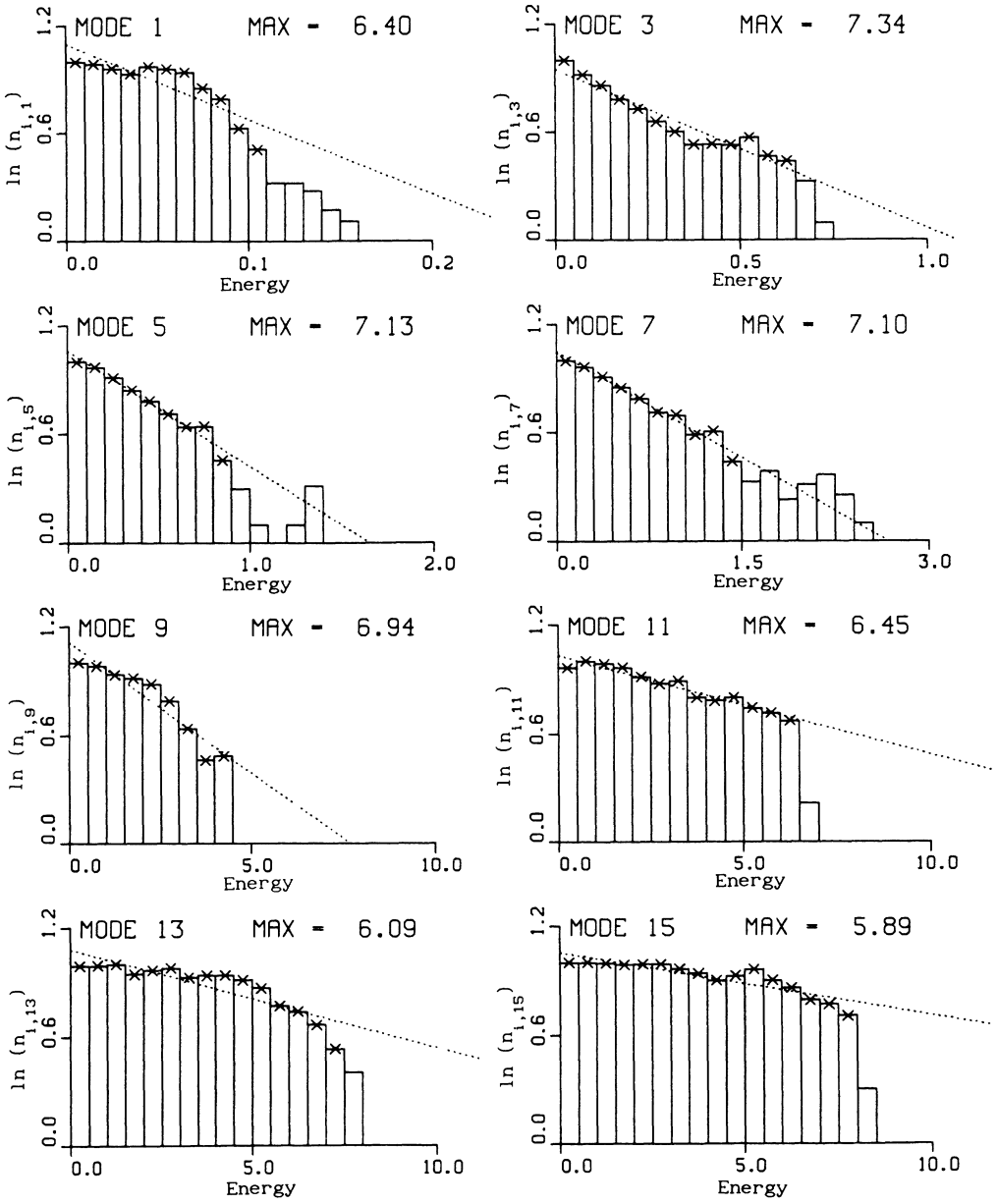

FIG. 3. Histograms of $\ln\left[\sum_{t=200}^{600} n_{i,s}(t)\right]$ vs energy for the odd modes $s=1,3,\ldots,15$. The dotted lines represent the best-fit straight lines through the points (marked by x) with sums greater than 20. The histogram data have been normalized to unity and the normalization constants are displayed at the tops of the graphs.

TABLE II. Maxwell-Boltzmann mode temperatures, from the time-ensemble mode energy distributions $\bar{\Theta}_s$ and from the statistical-ensemble mode energy distributions $\langle\bar{\Theta}_s\rangle$. Time-ensemble average mode energy $\bar{\varepsilon}_s$ and statistical-ensemble average mode energy $\langle\bar{\varepsilon}_s\rangle$.

s	$\bar{\Theta}_s$	$\langle\bar{\Theta}_s\rangle$	$\bar{\varepsilon}_s$	$\langle\bar{\varepsilon}_s\rangle$
1	0.04	0.01	0.04	0.01
3	0.15	0.08	0.12	0.08
5	0.22	0.21	0.22	0.24
7	0.36	0.36	0.37	0.33
9	1.00	1.26	1.22	1.44
11	2.83	2.21	2.17	2.10
13	3.03	3.22	2.72	2.90
15	4.90	3.54	3.14	2.89

TABLE III. Time-ensemble average kinetic mode temperature $\bar{\Theta}_s^k$ and statistical-ensemble average kinetic mode temperature $\langle\bar{\Theta}_s^k\rangle$.

s	$\bar{\Theta}_s^k$	$\langle\bar{\Theta}_s^k\rangle$
1	0.04	0.01
3	0.13	0.08
5	0.25	0.26
7	0.43	0.44
9	1.38	1.61
11	2.45	2.42
13	3.05	3.29
15	3.52	3.21

TABLE IV. Time-ensemble average kinetic particle temperature $\bar{T}_n^k$ and statistical-ensemble average kinetic particle temperature $\langle \bar{T}_n^k \rangle$.

n	$\bar{T}_n^k$	$\langle \bar{T}_n^k \rangle$
1	0.52	0.50
2	0.78	0.85
3	0.61	0.79
4	0.77	0.71
5	0.79	0.82
6	0.68	0.67
7	0.73	0.63
8	1.48	1.39

ergodic hypothesis and suggests that the statistical- and time-ensemble distribution functions for $\dot{q}_s^2$ (and for $\dot{x}_n^2$) are the same. We hope to report on an investigation of these distributions at a later date.

We remarked above that the time dependence of the mode energies in the irreversible region above 600 sec showed some sign of energy equipartition. To put this comment on a more quantitative footing, consider the time average of the mode energies $\varepsilon_s(t)$ in the ten time ranges $[100n \le t \le 100(n+1)]$ with $n=0,1,2,\ldots,9$. These data are plotted as a function of mid-interval time $100(n+1/2)$ for all 15 modes in Fig. 4. Below 600 sec there are large fluctuations in the averages for the odd mode energies and the even mode energies do not show on this scale. There is no indication of energy equipartition even among the odd modes alone. Above 600 sec the picture changes; the even mode energies appear at the expense of the odd mode energies; the fluctuations are smaller and the average energy plots suggest a tendency for most of the mode-energy averages to fluctuate about the equipartition value of $E_0/15=0.67$, the horizontal dashed line in Fig. 4. We conclude from this evidence that for the starting condition used in generating the time-ensemble data the chain does not exhibit energy equipartition in the reversible statistical equilibrium regime; energy equipartition only occurs as a result of contamination of the data by round-off errors.[16–18]

III. ACCURACY

Our discussion of the accuracy of our data has so far been confined to the error in the total energy (less than 0.02%) and the presence of round-off error as shown by the appearance of the forbidden even modes. In this section we extend the discussion to the errors in the position and velocity coordinates of the particles of the chain. Before we do this a few remarks on the Γ space of the system and the phenomenon of exponentially diverging trajectories (EDT) are appropriate.

The dynamical behavior of the chain can be fully described in terms of the motion of the phase point

$$(x_1,x_2,\ldots,x_N,\dot{x}_1,\dot{x}_2,\ldots,\dot{x}_N)\equiv(x_n,\dot{x}_n)$$

in the $2N$-dimensional Γ space of the system. For a given excitation of the chain, the phase point follows a path in Γ space. This path lies on the appropriate constant-

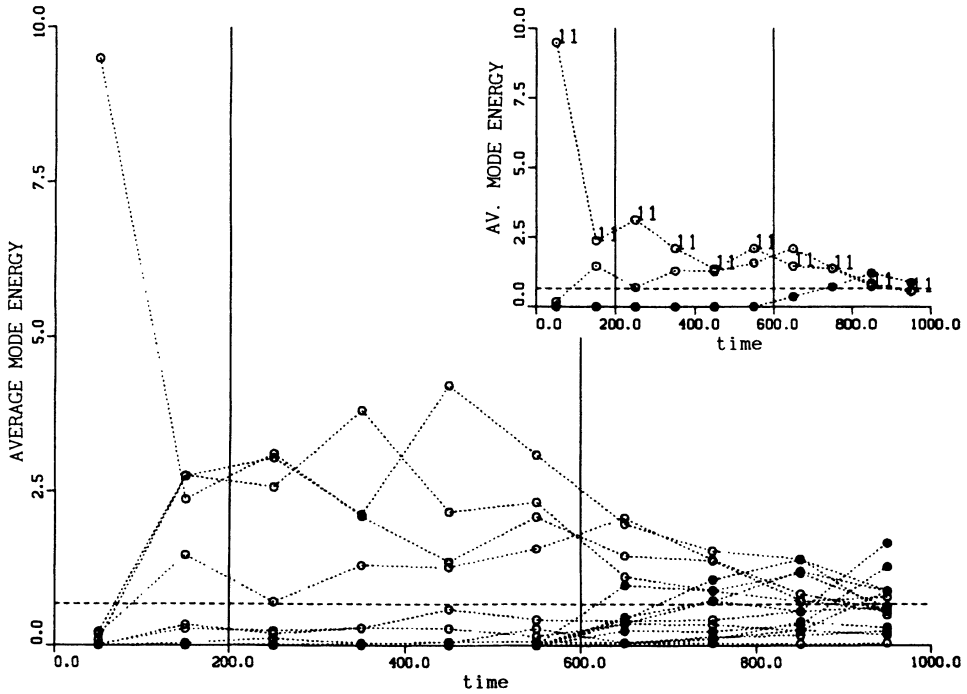

FIG. 4. Plot of the mode-energy averages in the time intervals $100n < t < 100(n+1)$, $n=0,1,2,\ldots,9$ vs the mid-interval time $100(n+\frac{1}{2})$. Empty (solid) circles represent the odd (even) mode values. The vertical lines pass through the two times 200 and 600 sec. The horizontal dashed line indicates the position of the equipartition values $E_0/15=0.67$. The inset shows more clearly the detailed behavior of the data for the three modes $s=9$, $s=10$, and $s=11$.

energy surface E_0 and is described by the set of $2N$ functions $(x_n(t),\dot{x}_n(t))$. For two different histories starting at two different points in Γ space, there result two nonintersecting paths $(x_n(t),\dot{x}_n(t))$ and $(x'_n(t),\dot{x}'_n(t))$, say. At a time t the distance between the two corresponding points on the two orbits is given by $L(t)$, where

$$L(t)^2=\sum_{n=1}^{N}\{[x_n(t)-x'_n(t)]^2+[\dot{x}_n(t)-\dot{x}'_n(t)]^2\} . \quad (11)$$

It is known that the equations of motion (2) exhibit the property of EDT,[18] that is to say, if two *closely* spaced starting points are chosen, then $L(t)$ increases, on average, exponentially with increasing time. This behavior cannot continue indefinitely because both the kinetic energy and the physical size of the system are bounded. Typically we might expect $L \lesssim 2\sqrt{E_0}$.

To carry out the numerical integration of equations of motion such as (2), one chooses an algorithm and a step size h (or iteration frequency $1/h$). The algorithm converges to the exact solution as $h \to 0$ and so one expects that the smaller the h the smaller the truncation error and hence the more accurate the numerical solution. However, with increasing iteration frequency significant round-off error occurs earlier and earlier in the calculation. Thus the choice of h in practice involves a trade-off between small truncation error and length of record free of appreciable round-off error. As discussed previously, Sec. II above (see also Ref. 1), the energy in the forbidden even modes provides us with a quantitative measure of the presence of round-off error. To estimate the numerical accuracy (i.e., truncation error) of our histories in a time regime in which the round-off error is negligible we use the smaller-the-h-the-more-accurate-the-solution property of the algorithm. However, complications and limitations arise because of the occurrence of EDT. These come about as follows. Suppose we choose a starting condition and calculate the numerical record $(x_n(t),\dot{x}_n(t))$ for a step size h, we repeat this process for the *same starting condition* and a smaller step size h' to get the record $(x'_n(t),\dot{x}'_n(t))$. Now, while the starting point is the same for these two records, the difference in truncation error (since $h \neq h'$) leads to a divergence of the histories—a divergence which can be measured by the corresponding distance $L(t)$. The truncation divergence is in turn amplified by the exponential divergence *intrinsic* to the equations of motion (2). The exponential divergence of trajectories is a global property of the equations of motion. In a local region of phase space, trajectories through nearby points do not diverge exponentially—this result is proved in the Appendix. It follows that the global divergence property cannot be avoided simply by choice of algorithm that has high local accuracy. In Fig. 5 we have drawn the separation function $L(t)$ in the time interval (0,600) for two numerical histories of the $15+2$ particle chain. Each history has the starting excitation discussed in earlier sections (i.e., the q_{11} mode displaced from rest); they differ only in the time steps $h=0.01$ and $h'=0.005$. On the semilog plot we see the initial average exponential rise in L followed by fluctuations about the saturation value $2\sqrt{E_0}$. The curve reaches 1% of the saturation value at $t=164$ sec and then rises rapidly to its long-term behavior. We interpret this graph as indicating that the $h=0.01$ history is accurate to better than 1% only over the range (0,164) and that at later times there is a rapid deterioration in its accuracy. In light of these remarks, it is clear that the $h=0.01$ history is not a good representation of the exact history over the whole

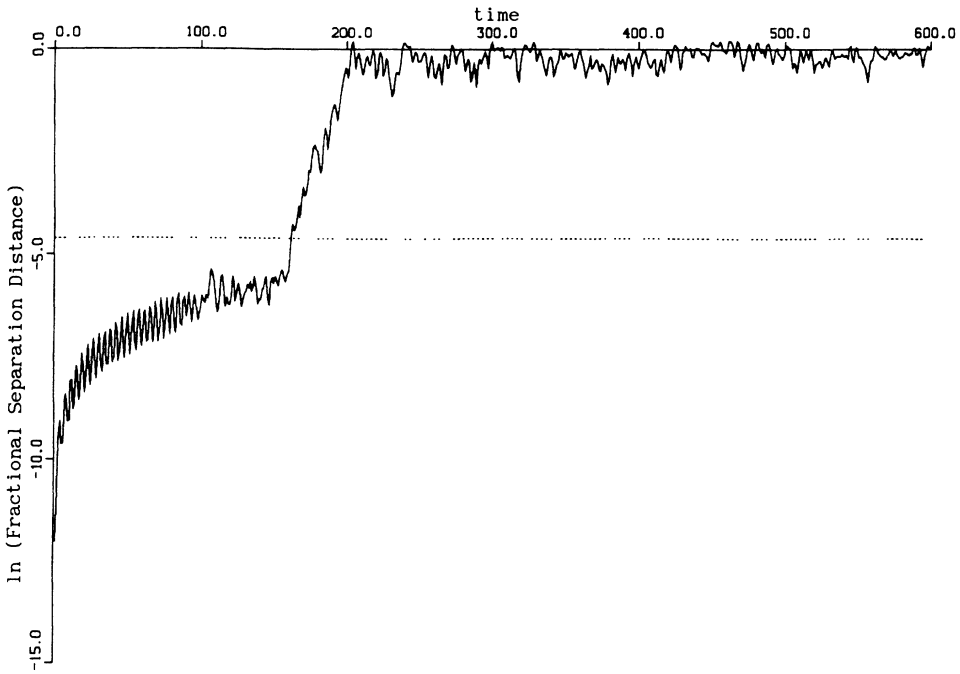

FIG. 5. Graph of the separation function $L(t)$, Eq. (11), for the same starting state but different step sizes $h=0.01$, $h'=0.005$.

range (0,600)—merely the first 164 sec. Further calculations show that the $h=0.005$ history is no better; while it cuts the 1% line relative to the $h=0.0025$ history at a later time of 175 sec, the corresponding even-mode-energy curve cuts the total-energy error curve as expected at an earlier time of 500 sec, i.e., an improvement in truncation error at the expense of the length of the round-off error-free time interval. By considering smaller and smaller h values we then conclude that we cannot get a representation of the q_{11} excitation to better than 1% outside a range of about 300 sec for the case of the fourth-order predictor-corrector algorithm[12,13] plus quadruple precision. We have also briefly looked at other algorithms and found very similar results.[19] In summary, then, there is a practical barrier to accurate long-time numerical integrations of the equations of motion (2). This barrier of 300 sec in quadruple precision is too short to provide enough data in a single history to test for a Maxwell-Boltzmann distribution and hence test for the ergodic property in the exact solution. Returning to the discussion of the reversible $h=0.01$, 600-sec data of Sec. II, we now consider the question of just how one should regard the agreement between the statistical- and time-ensemble data reported above. Our results can be interpreted in the following two quite different ways.

First of all, consider Fig. 6. Here we have calculated $L(t)$ for $h=0.01$ and $h'=0.005$ as above, Fig. 5, but only for the time interval (0,50). At $t=50$ the $h=0.01$ integration continues but the $h'=0.005$ integration is restarted with the $t=50$, $h=0.01$ data as initial values. This process is continued at 50-sec intervals until the end of 600 sec. The resulting sawtooth $L(t)$ is shown in Fig. 6. The dashed line represents the 1% value. We interpret this graph as follows. In the interval (0,50) the integration data lie close (better than 1%) to the exact path l_1, say, in Γ space; beyond this time, while the data deviates to a larger and larger extent from l_1, Fig. 5, the graph in Fig. 6 indicates that it gives a good representation of another path l_2 for the next 50 sec. Continuing in this fashion we see that the data closely represent a series of segments of different paths $l_1, l_2, \ldots, l_{12}$. None of these exact paths can have the same starting point or indeed a common point. It is clear from Fig. 5 that l_n provides a poorer representation of the path of interest l_1 with increasing n. On the basis of these remarks, we may think of our $h=0.01$ data as a series of 50-sec samplings from various exact paths on the energy surface[20] $E_0=10$. Since these are samplings from *different* paths at *different* times, the agreement between the mode-energy distributions described above and those for the statistical ensemble,[1] cannot be regarded as *proof* that the ergodic hypothesis holds for some exact solution. The agreement merely indicates that two different sampling techniques on the energy surface give the same Maxwell-Boltzmann distributions for the exact solutions to Eqs. (2). In this interpretation it is nevertheless interesting that the distributions from a large number of samples (101) in the statistical ensemble agree with distributions from a small number of samples (8) in the time ensemble.

The second way of looking at our $h=0.01$ data starts with the observation that, in choosing an nth-order predictor-corrector algorithm and step size h, one replaces the differential equations of motion with a set of nonlinear, coupled difference equations. In the absence

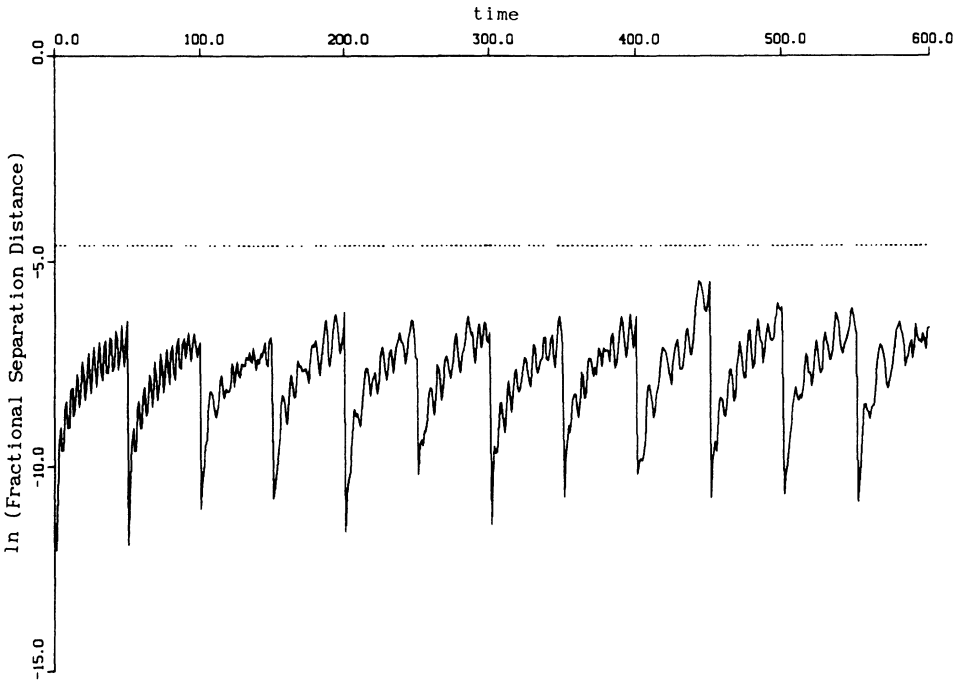

FIG. 6. Graph of the separation function $L(t)$, Eq. (11), for step sizes $h=0.01$ and $h'=0.005$. The integration is restarted for the smaller step size at 50-sec intervals using the $h=0.01$ data.

of round-off error the computed numerical data represent precisely the *exact* solution to the difference equations—for a given choice of step h and algorithm, order n, the computer calculates the resulting difference equation solution $(x_n(mh),\dot{x}_n(mh))$ at the M time points $mh, m=1,2,\ldots,M$. Thus, in the case of the fourth-order predictor-corrector algorithm with step $h=0.01$, we have obtained *exact difference equation data* for (a) 101 different histories, the statistical ensemble of Ref. 1, and (b) a single history over a much longer interval, the time ensemble of the present paper. In the equilibrium regime the mode-energy distribution functions for the two ensembles are found to be of Maxwell-Boltzmann form with the same set of mode temperatures, Sec. II above. This means, in particular, that an average over copies is equal to an average over the time variable mh, i.e., the *ergodic hypothesis holds for the nonlinear, coupled difference equations.* As remarked previously, we have obtained similar results for other algorithms [i.e., other nonlinear coupled difference equations representing Eqs. (2)] and so we believe that the ergodic property found in the difference equation data is a result of the ergodic nature of the differential equations (2). In view of the barriers to accurate long-time numerical integrations of the equations of motion (2) discussed above, it appears that a *direct* proof of the ergodic behavior of Eqs. (2) can come only from an algebraic analysis and not a numerical treatment.

Note that the property of Maxwell-Boltzmann distributions, in contrast to the ergodic property, can be attributed directly to the differential equations of motion because of the first interpretation of the data as being a set of accurate samplings of exact paths on the energy surface E_0.

IV. COMMENTS

Our numerical data for the statistical ensemble[1] and for the time ensemble suggest that there is an ergodic region or "sea" (described by Maxwell-Boltzmann functions for at least some physical properties) on the constant-energy surface $E_0=10$ for the quartic Fermi-Pasta-Ulam (FPU) chain. We have no evidence to show whether the statistical- and time-ensemble data cover partially or completely overlapping regions in this sea. We have no evidence for the extent of the sea. We think it is extremely unlikely that access to this sea is confined to the small set of paths passing through our 101 initial states. We expect to find ergodic and Maxwell-Boltzmann properties in the system for a wide range of starting conditions on this energy surface and indeed we expect other nonlinear particle systems to exhibit the same type of behavior.

ACKNOWLEDGMENTS

This work was supported by the National Sciences and Engineering Research Council of Canada, and the University of Waterloo.

APPENDIX

We write the particle equations of motion (2) as the autonomous first-order system

$$\frac{d\mathbf{X}}{dt}=\mathbf{F}(\mathbf{X}(t)) , \tag{A1}$$

where $\mathbf{X}(t)$ and $\mathbf{F}(\mathbf{X}(t))$ are $2N$-dimensional column vectors:

$$\mathbf{X}=(x_1,x_2,\ldots,x_N,\dot{x}_1,\dot{x}_2,\ldots,\dot{x}_N)^T , \tag{A2}$$

$$\mathbf{F}=(\dot{x}_1,\dot{x}_2,\ldots,\dot{x}_N,x_1,x_2,\ldots,x_N)^T . \tag{A3}$$

Consider two nearby points in phase space $\mathbf{X}_0(0)$ and $\mathbf{X}_1(0)$ such that $\mathbf{X}_1(0)=\mathbf{X}_0(0)+\Delta X(0)$, where $|\Delta X(0)| \ll 2\sqrt{E_0}$. Trajectories $X_0(t),X_1(t)$ passing through these nearby points separate in time. To first order the separation distance $\Delta X(t)$ satisfies the variational equation

$$\frac{d\Delta X}{dt}=\underline{A}(\mathbf{X}_0(t))\Delta X , \tag{A4}$$

where the stability matrix $\underline{A}$ has components

$$A_{ij}(t)=\left.\frac{\partial F_i}{\partial X_j}\right|_{\mathbf{X}_0(t)} . \tag{A5}$$

To examine the *short-time* divergence of trajectories around a particular point $X_0^*=X_0(t^*)$, say we make the further simplifying short-time approximation $\underline{A}(X_0(t))\approx\underline{A}(X_0^*)$ (Ref. 21) in Eq. (A5). If $\underline{A}(X_0^*)$ has $2N$ distinct nonvanishing eigenvalues $\lambda_1,\lambda_2,\ldots,\lambda_{2N}$ with eigenvectors $\mathbf{E}_1,\mathbf{E}_2,\ldots,\mathbf{E}_{2N}$, then the solution to the variational equation can be written in the form[22]

$$\Delta X(t)=\sum_{i=1}^{2N}\Delta X(0)e^{\lambda_i t}\mathbf{E}_i(X_0^*) . \tag{A6}$$

Thus two trajectories through nearby points in phase space diverge exponentially for short times if and only if at least one of the eigenvalues of the matrix $\underline{A}(X_0^*)$ has a real and positive component. In the following we show that in the case of the quartic FPU chain[23] the $2N$ eigenvalues of the matrix $\underline{A}(X_0^*)$ are *all* purely imaginary at *every point* in phase space. Thus the average exponential divergence of trajectories reported in Sec. III is a global divergence and is not an average of local exponential divergences.

The stability matrix $\underline{A}$ consists of four $N\times N$ blocks:

$$\underline{A}_{2N\times 2N}=\begin{bmatrix}\underline{\varnothing}_{N\times N} & \underline{I}_{N\times N}\\ \underline{B}_{N\times N} & \underline{\varnothing}_{N\times N}\end{bmatrix} , \tag{A7}$$

where $\underline{\varnothing}_{N\times N}$ is an $N\times N$ matrix with all elements identically zero, $\underline{I}_{N\times N}$ is the $N\times N$ identity matrix, and $\underline{B}_{N\times N}$ is the $N\times N$ symmetric tridiagonal matrix:

$$\underline{B}_{N\times N}=\begin{bmatrix} -(b_0+b_1) & b_1 & 0 & \cdots & 0 & 0 & 0 \\ b_1 & -(b_1+b_2) & b_2 & \cdots & 0 & 0 & 0 \\ 0 & b_2 & -(b_2+b_3) & \cdots & 0 & 0 & 0 \\ \vdots & \vdots & \vdots & & \vdots & \vdots & \vdots \\ 0 & 0 & 0 & \cdots & b_{N-2} & -(b_{N-2}+b_{N-1}) & b_{N-1} \\ 0 & 0 & 0 & \cdots & 0 & b_{N-1} & -(b_{N-1}+b_N) \end{bmatrix}, \tag{A8}$$

with

$$b_r=1+3\mu(x_{r+1}-x_r)^2 . \tag{A9}$$

It is an easy matter to show that the $2N$ eigenvalues of the stability matrix $\underline{A}$ are related to the N eigenvalues $\omega_1,\omega_2,\ldots,\omega_N$ of the symmetric tridiagonal matrix $\underline{B}$ by $\lambda=\pm\sqrt{\omega}$. Furthermore, since the eigenvalues of a real symmetric matrix are all real and distinct it remains to show that the eigenvalues of $\underline{B}$ are all negative. We define a Sturm series $f_N(\omega),f_{N-1}(\omega),\ldots,f_0(\omega)$ for $\underline{b}$ as follows:[24]

$$f_N(\omega)\equiv|\underline{B}-\omega\underline{I}|=0 , \tag{A10}$$

$$f_0(\omega)=1 , \tag{A11}$$

$$f_1(\omega)=-(b_0+b_1)-\omega , \tag{A12}$$

$$\vdots$$

$$f_r(\omega=-(b_{r-1}+b_r+\omega)f_{r-1}(\omega) -b_{r-1}^2 f_{r-2}(\omega) . \tag{A13}$$

It follows from Gerschgorin's theorem[25] that all the eigenvalues of $\underline{B}$ lie in the range

$$-2(b_j+b_{j-1})\le\omega\le+2(b_j+b_{j-1}) , \tag{A14}$$

where the index j is that index for which b_j+b_{j-1} is a maximum. Sturm's theorem now tells us that the number of distinct real roots in the interval $-2(b_j+b_{j-1})\le\omega\le0$ is equal to the number of changes of sign in the sequence $f_N(0),f_{N-1}(0),\ldots,f_1(0),f_0(0)$. Substituting $\omega=0$ into Eqs. (A10)–(A13) we have

$$f_0(0)=1 , \tag{A15}$$

$$f_1(0)=-(b_0+b_1) , \tag{A16}$$

$$f_2(0)=+(b_1b_2+b_1b_0+b_2b_0) , \tag{A17}$$

$$f_3(0)=-(b_1b_2b_3+b_3b_2b_0+b_2b_1b_0+b_0b_1b_3) , \tag{A18}$$

$$\vdots$$

$$f_N(0)=-(b_Nb_{N-1}\cdots b_0) . \tag{A19}$$

Since $b_r>0$ for all r[23] there are N changes of sign and hence $\underline{B}$ has N distinct *negative* real eigenvalues.

*Present address: Department of Theoretical Physics, Research School of Physical Sciences, The Australian National University, Canberra, Australian Capital Territory 2601, Australia.

[1]B. I. Henry and J. Grindlay, Phys. Lett. **A19**, 215 (1986); see also B. I. Henry and J. Grindlay, Physica **28D**, 49 (1987).

[2]We shall adopt the nomenclature of Pauli [W. Pauli, *Pauli Lectures on Physics: Volume 4, Statistical Mechanics,* edited by C. P. Enz (MIT Press, Cambridge, MA, 1973), p. 21] and refer to the collection of data in a single history as a "time ensemble" and the collection of data in a set of histories as a "statistical ensemble."

[3]R. C. Tolman, *The Principles of Statistical Mechanics* (Oxford University Press, Oxford, 1938), pp. 96 and 82.

[4]D. ter Haar, Revs. Mod. Phys. **27**, 289 (1955).

[5]E. Fermi, J. Pasta, and S. Ulam, *Nonlinear Wave Motion,* Vol. 15 of *Lectures in Applied Mathematics,* edited by A. C. Newell (American Mathematical Society, Providence, 1974), p. 143.

[6]M. Henon and C. Heiles, Astron. J. **69**, 73 (1964).

[7]M. C. Carotta, C. Ferrario, G. Lo Vecchio, and L. Galgani, Phys. Rev. A **17**, 786 (1978).

[8]G. Contopoulos, L. Galgani, and A. Giorgilli, Phys. Rev. A **18**, 1183 (1978).

[9]N. Saito and A. Ichimura, *Stochastic Behavior in Classical and Quantum Hamiltonian Systems,* Vol. 93 of *Lecture Notes in Physics,* edited by G. Casati and J. Ford (Springer-Verlag, New York, 1979), p. 137.

[10]G. Benettin, G. Lo Vecchio, and A. Tenenbaum, Phys. Rev. A **22**, 1709 (1980).

[11]A. Malagoli, G. Paladin, and A. Vulpiani, Phys. Rev. A **34**, 1550 (1986).

[12]D. Beeman, J. Comput. Phys. **20**, 130 (1976).

[13]A. R. Janzen and J. W. Leech, Comput. Phys. Commun. **32**, 349 (1984).

[14]In Ref. 1 we used time averaging over copy histories to calculate the slope—we indicate this in Tables II–IV by using the short horizontal bar.

[15]We have been unable to write down a form for the distribution function for a cell in the Γ space of this system [the vastly different mode temperatures associated with different portions of the shared anharmonic energy term (5) indicate that

it cannot be Maxwell-Boltzmann] and so we are not in a position to argue algebraically that the mode temperature Θ_s and the kinetic temperature $\overline{\Theta}_s^k$ of a given mode should be the same, as the numerical evidence in Tables II and III suggest.

[16]N. Ooyama, H. Hirooka, and N. Saito, J. Phys. Soc. Jpn. **27**, 815 (1969).

[17]N. Saito, N. Ooyama, Y. Aizawa, and H. Hirooka, Suppl. Prog. Theor. Phys. **45**, 209 (1970).

[18]N. Saito, N. Hirotomi, and A. Ichimura, J. Phys. Soc. Jpn. **39**, 1431 (1975).

[19]We have used a number of other algorithms, viz., Runge-Kutta, the half-step method and Butcher's fifth-order method, to integrate the equations of motion (2). In each case we calculated total-energy error, even-mode-energy error and L curves. Patterns of behavior similar to what have been reported above were seen in the case of each algorithm we explored. In addition, calculations of average mode energies in the equilibrium regime yielded numbers in agreement with those in Table II.

[20]See similar remarks by J. Ford in *Chaotic Dynamics and Fractals,* edited by M. F. Barnsley and S. G. Demko (Academic, New York, 1986), p. 39.

[21]Toda [M. Toda, Phys. Lett. **48A**, 335 (1984)] originally employed this approximation to identify conditions for the onset of stochastic motion in a Hamiltonian system. The quartic FPU chain[23] is another counterexample to the Toda criterion.

[22]See, for example, L. A. Pipes and L. R. Harvill, *Applied Mathematics for Engineers and Physicists* (McGraw-Hill, New York, 1970), p. 122.

[23]This property is common to all anharmonic chains with nearest-neighbor linear and nonlinear forces where the nonlinear interatomic potential $V(r_j)$ (r_j is the relative displacement of neighboring atoms) satisfies the condition $d^2V/dr_j^2 > -1$ for all r_j.

[24]See, for example, S. J. Hammarling, *Latent Roots and Latent Vectors* (University of Toronto, Toronto, 1970), Chap. 5.

[25]See Ref. 24, Chap. 1.